



RESEARCH ARTICLE

10.1002/2016RS005973

Key Points:

- A compact planar antenna is proposed which is based on two pairs of meandered line loops that are interconnected to each other
- The antenna's characteristics can be controlled by modifying the meandered line parameters
- The proposed meandered antenna is easy to fabricate and its low profile makes it suitable for wireless portable devices

Correspondence to:

M. Naser-Moghadasi,
mn.moghaddasi@srbiau.ac.ir

Citation:

Alibakhshi-Kenari, M., M. Naser-Moghadasi, R. A. Sadeghzadeh, B. S. Virdee, and E. Limiti (2016), A new planar broadband antenna based on meandered line loops for portable wireless communication devices, *Radio Sci.*, 51, 1109–1117, doi:10.1002/2016RS005973.

Received 6 FEB 2016

Accepted 23 JUN 2016

Accepted article online 27 JUN 2016

Published online 23 JUL 2016

A new planar broadband antenna based on meandered line loops for portable wireless communication devices

Mohammad Alibakhshi-Kenari¹, Mohammad Naser-Moghadasi¹, R. A. Sadeghzadeh², Bal S. Virdee³, and Ernesto Limiti⁴

¹Faculty of Engineering, Science and Research Branch, Islamic Azad University, Tehran, Iran, ²Faculty of Electrical Engineering, K. N. Toosi University of Technology, Tehran, Iran, ³Center for Communications Technology, Faculty of Life Sciences and Computing, London Metropolitan University, London, UK, ⁴Dipartimento di Ingegneria Elettronica, Università degli Studi di Roma Tor Vergata, Roma, Italy

Abstract This article presents the design of a novel planar antenna structure comprising two pairs of interconnected meandered line loops that are grounded to a truncated *T*-shaped ground plane through two via holes. The *T*-shaped ground plane is used as a reflector to enhance the performance of the antenna. The resulting antenna is compact occupying an area of $38.5 \times 36.6 \text{ mm}^2$ ($0.070\lambda_0 \times 0.067\lambda_0$), where free-space wavelength is 550 MHz. The antenna radiates omnidirectionally in the *E* plane across its operational bandwidth (550 MHz to 3.85 GHz) with peak gain and efficiency of 5.5 dBi and 90.1%, respectively, at 2.35 GHz and reflection coefficient better than -10 dB . These characteristics make the antenna suitable for numerous applications, in particular, JCDMA, UHF RFID, GSM 900, GPS, KPCS, DCS, IMT-2000, WiMAX, WiFi, and Bluetooth.

1. Introduction

Low-profile antennas are in high demand for handheld and portable wireless devices; however, the major drawback of many such antenna designs is their narrow impedance bandwidth. Some antennas designs are impractical as they can scarcely cover the bandwidth requirement which is needed to accommodate potential detuning effects due, for example, to the presence of a human operator. Furthermore, the market trend of personal wireless devices is moving toward a universal system that can be used anywhere. Rapid expansion of the wireless communication industry has created a need for connectivity among various wireless devices using short range wireless links in the Bluetooth operating band to get rid of the cable connections. This requires therefore multiple frequency band operation. Dual-band and tri-band compact antennas have been realized to help the transition of new wireless system generations go smoothly, but the current market demand needs wireless systems to operate in more than three bands [Alibakhshi-Kenari et al., 2016a; Alibakhshi-Kenari et al., 2016b; Alibakhshi-Kenari et al., 2016c; Alibakhshi-Kenari et al., 2015b; Alibakhshi-Kenari et al., 2015c; Alibakhshi-Kenari et al., 2015d; Alibakhshi-Kenari et al., 2016d; Alibakhshi-Kenari et al., 2016e; Alibakhshi-Kenari and Naser-Moghadasi, 2015; Alibakhshi-Kenari et al., 2015a; Alibakhshi-Kenari et al., 2016f].

It is well known that monopole antennas exhibit better bandwidth characteristic over the conventional microstrip antennas. Although monopole antennas can achieve multiple frequency operation, they are, however, relatively large in size [Abutarboush et al., 2012; Sharma and Hashmi, 2014]. Feasibility of reducing the antenna size by meandering the geometry of the antenna structure has been demonstrated previously [Chien et al., 2013; Ojaroudi et al., 2012; Pandeewari and Raghavan, 2015; Li et al., 2013; Lee et al., 2014]. In Pandeewari and Raghavan [2015] a compact monopole antenna is reported for Radio Frequency Identification (RFID) application at 5.8 GHz, where a meandered coplanar waveguide (CPW) feed line is used to excite a hexagonal split ring resonator. It is shown that the meandered CPW feed line also improves the impedance matching of the antenna. The measured impedance bandwidth of the antenna is from 5.4 to 6.0 GHz for return loss $< -10 \text{ dB}$. A dual-band, meandered monopole antenna reported in Li et al. [2013] is applicable for WLAN/WiMAX systems. The antenna consists of an asymmetric ground plane, an asymmetric coplanar strip fed structure, and coupled meandered monopole type of radiating elements that are designed to operate at 3.5 and 5.8 GHz. The two resonance frequencies of the antenna can be controlled by adjusting the dimensions of the meandered monopoles. In Lee et al. [2014] a meandering dipole patch antenna is presented for a sensor node in a wireless network system. The antenna without a matching circuit covers the UHF band frequency (405–425 MHz). The authors have shown the meandering dipole structure can be reduced in size to $\lambda/6$ at 415 MHz. The resonant frequency of the antenna can be adjusted by changing the antenna geometry. The maximum gain of the antenna is limited to

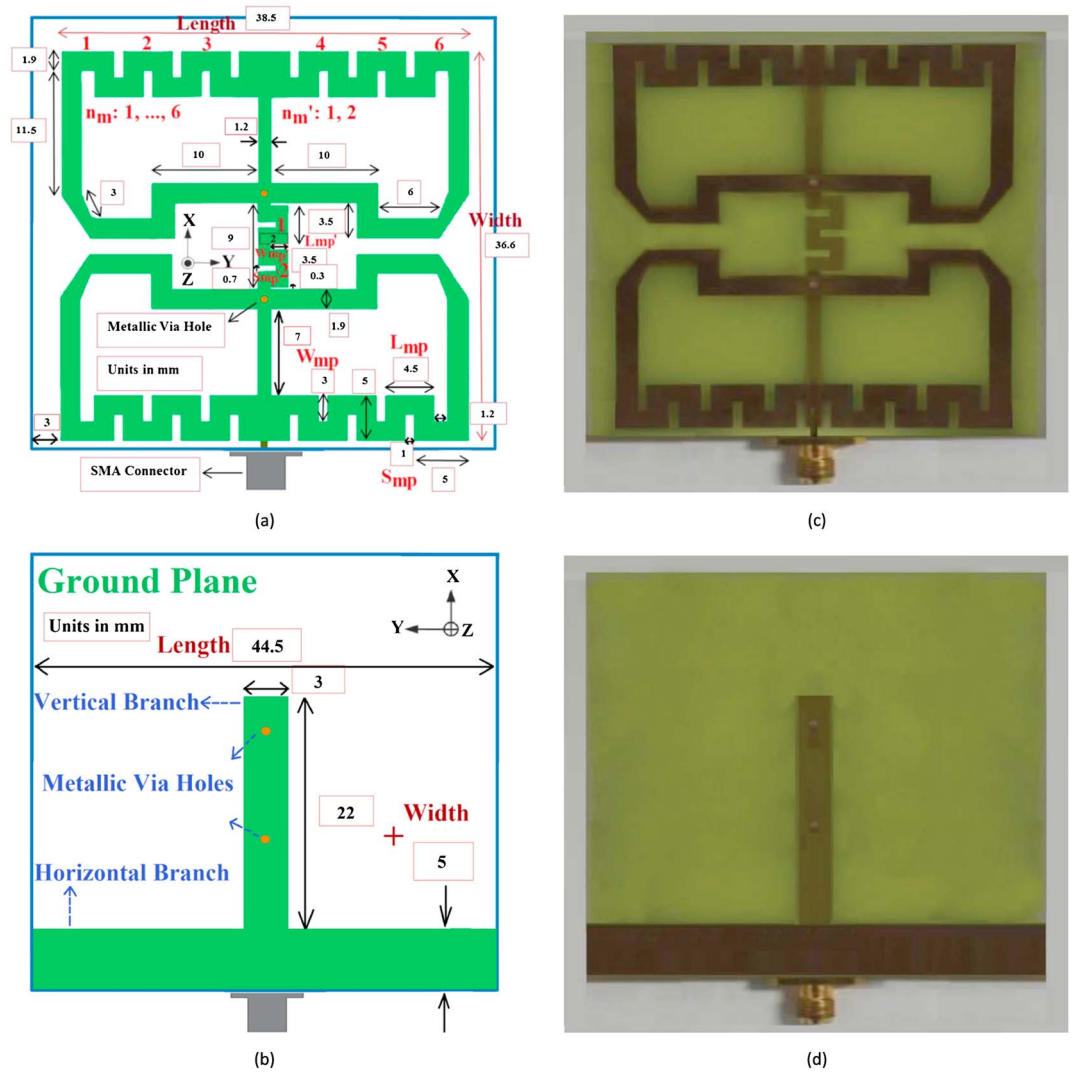


Figure 1. Geometry and prototype of the proposed meandered antenna (dimensions in millimeters): (a) top layer, (b) bottom layer, (c) fabricated prototype (top layer), and (d) fabricated prototype (bottom layer).

0.94 dBi at 420 MHz. Although the aforementioned meandered antennas are relatively small in size their operational bandwidth is however limited.

This paper presents a planar antenna that has a wide bandwidth, low profile, and is compact in size. The antenna consists of two pairs of interconnected meandered loops, i.e., two main and one auxiliary, and a truncated ground plane. The antenna is optimized for the operation over 550 MHz to 3.85 GHz. The planar antenna can be easily constructed and occupies an area of $38.5 \times 36.6 \text{ mm}^2$. The antenna design was analyzed using a commercial an Electromagnetic (EM) solver (HFSS™). The measured results confirm the proposed antenna has well-defined omnidirectional radiation patterns and its gain and efficiency span $0.84 \text{ dBi} \leq \text{gain} \leq 5.5 \text{ dBi}$ and $21.1\% \leq \text{efficiency} \leq 90.1\%$, respectively.

2. Proposed Antenna Configuration

Configuration of the proposed antenna, shown in Figure 1, consists of four meandered line loops, where each pair of loop has a common side. The upper and lower pair of loops is in close proximity to each other and is directly interconnected to each other with a meandered line. Sections of the upper and lower pairs of loops are strongly coupled to each other. The antenna is grounded through two via holes at the interconnecting points. The ground plane is truncated in an inverted T shape. The antenna was designed on a 0.8 mm

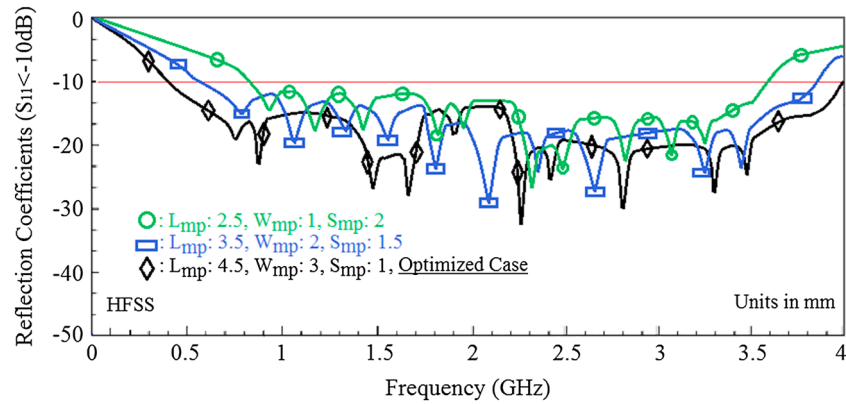


Figure 2. Effect of varying length, width, and space of the meandered parameters (L_{mp} , W_{mp} , and S_{mp}) on the reflection coefficient while keeping all the other parameters fixed in Figures 1.

Rogers RO4003 substrate with a dielectric constant $\epsilon_r = 3.38$ and loss tangent $\tan \delta = 0.0022$. The overall dimensions of the antenna are $38.5 \times 36.6 \text{ mm}^2$ ($0.070\lambda_0 \times 0.067\lambda_0$), where free-space wavelength (λ_0) is 550 MHz. The optimized antenna parameters in Figure 1 were obtained using the commercial EM solver HFSS (high-frequency structure simulator) based on the finite-element method. The goal of the optimization was to achieve excellent characteristics in terms of impedance match, operational bandwidth, radiation patterns, and reduction in antenna size for integration in wireless portable communications devices.

The T-shaped ground plane essentially acts like a reflector. In addition to the surface waves which are excited over the antenna, the strong near-field coupling between the meandered line loops and the reflector element help to improve the impedance matching of the antenna over its operational bandwidth. It is evident from the surface current distribution simulation results, which are presented later, that the effect of the reflector is more pronounced at lower frequencies than at higher frequencies. The optimized antenna structure excites resonances over its wide bandwidth extending from 500 MHz to 3.85 GHz, which makes it suitable for numerous wireless systems.

The dimensions and shape of the meandered lines and their spacing are key parameters that determine the antenna’s characteristics. The input impedance of meandered line sections is [Balanis, 1997; Du et al., 2015]

$$Z_{in} = jZ_0 \tan \left[K_n \sqrt{\epsilon_{re}} \left(L_{mp} + L'_{mp} \right) \right] \tag{1}$$

where K_n is the wave number in free space, ϵ_{re} is effective dielectric constant; L_{mp} is the length of the horizontal meander line section; and L'_{mp} is the length of the vertical interconnecting meander line section. The characteristic impedance of the meandered line is [Du et al., 2015]

$$Z_0 = \frac{\eta}{\pi} \cosh^{-1} \left(\frac{\alpha}{\beta} \right) \tag{2}$$

where α represents the gap between the meandered line sections, β represents the width of the meander line sections, and $\eta = \sqrt{\epsilon_{re}\mu_0}$ is the characteristic impedance. The above equations indicate the impedance of the antenna can be altered by changing the physical parameters (gap and width) of the meander lines.

3. Parametric Study and Measured Results

The geometry of the proposed antenna is complex to theoretically model; hence, it was necessary to undertake a parametric study in order to understand the key parameters that determine its performance.

Table 1. Effect of Meandered Line Parameters (L_{mp} , W_{mp} , and S_{mp}) on the Impedance Bandwidth for $S_{11} < -10 \text{ dB}$

Meander Lined Parameters (mm)	Frequency Span (GHz)	Impedance Bandwidth (GHz)	Fractional Bandwidth (%)
$L_{mp} = 2.5, W_{mp} = 1, S_{mp} = 2$	0.825–3.60	2.775	125.4
$L_{mp} = 3.5, W_{mp} = 2, S_{mp} = 1.5$	0.580–3.85	3.270	147.6
$L_{mp} = 4.5, W_{mp} = 3, S_{mp} = 1$	0.400–4.00	3.600	163.6

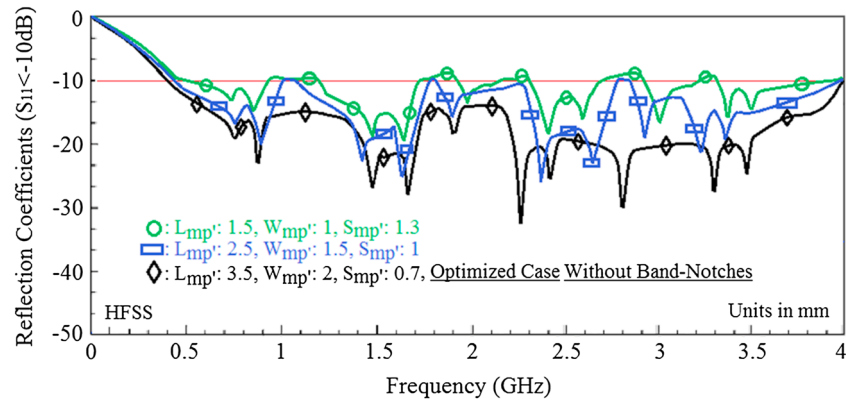


Figure 3. Effect of varying length, width, and space of the interconnecting meander line (L'_{mp} , W'_{mp} and S'_{mp}) on the proposed antenna’s impedance matching property while keeping all other parameters fixed as in Figures 1.

The effect of the meandered line length (L_{mp}), width (W_{mp}) and spacing (S_{mp}) on the impedance bandwidth of the antenna is shown in Figure 2. It is evident from the results that a larger value of L_{mp} and W_{mp} and a lower S_{mp} can greatly enhance the impedance match of the antenna. For $L_{mp} = 4.5$ mm, $W_{mp} = 3$ mm, and $S_{mp} = 1$ mm the impedance bandwidth is made to stretch from 0.4 to 4 GHz for $S_{11} < -10$ dB. The results are tabulated in Table 1.

The effect of the interconnecting meandered line parameters (L'_{mp} , W'_{mp} , and S'_{mp}) on the impedance match is shown in Figure 3. It reveals the impedance match is greatly improved by increasing L'_{mp} and W'_{mp} and decreasing S'_{mp} . For $L'_{mp} = 3.5$ mm, $W'_{mp} = 2$ mm, and $S'_{mp} = 0.7$ mm the impedance bandwidth extends to 3.59 GHz. Lower values of L'_{mp} and W'_{mp} and higher S'_{mp} result in a reflection coefficient response with band notches. Results are tabulated in Table 2.

The number of turns used in the meandered lines on the antenna’s reflection coefficient response was also investigated. Figure 4 shows that the number of resonance responses increase with the number of meandered line turns, where the turns for the main and interconnecting meandered lines are represented by n and n' , respectively. Results reveal a higher number of turns can substantially improve the impedance bandwidth of the antenna. The impedance bandwidth improves from $BW = 121.9\%$ for $n = 2$ and $n' = 0$ (with no interconnecting meandered line) up to $BW = 163.6\%$ for $n = 6$ with interconnecting meandered line implemented using two turns ($n' = 2$).

The antenna in Figure 1 was fabricated to verify its performance. The antenna’s far-field characteristics were measured in anechoic chamber using the measurement system NSI300V-30X30 and Agilent 8722ES series vector network analyzer. The antenna’s simulated and measured reflection coefficient response is shown in Figure 5a. There is good agreement between the measured and simulated results. The discrepancy in the results is due to manufacturing tolerance and unaccounted losses in the surface roughness of the patch.

Table 2. Effect of Interconnecting Meandered Line Parameters (L'_{mp} , W'_{mp} , and S'_{mp}) on Band Notches and Impedance Matching for $S_{11} \leq -10$ dB

Interconnecting Meandered Line Parameters (mm)	Span of Notched Bands (GHz)	Impedance Bandwidth (GHz)/Frequency Range (GHz)
$L'_{mp} = 1.5, W'_{mp} = 1, S'_{mp} = 1.3$	NB#1: 0.93–1.20	0.40/(0.52–0.92)
	NB#2: 1.71–1.92	0.53/(1.21–1.74)
	NB#3: 2.12–2.30	0.17/(1.97–2.14)
	NB#4: 2.69–2.91	0.34/(2.35–2.69)
	NB#5: 3.20–3.31	0.26/(2.95–3.21)
$L'_{mp} = 2.5, W'_{mp} = 1.5, S'_{mp} = 1$	NB#1: 1.00–1.10	0.47/(3.33–3.80)
	NB#2: 1.78–1.81	0.55/(0.46–1.01)
	NB#3: 2.78–2.84	0.69/(1.10–1.79)
$L'_{mp} = 3.5, W'_{mp} = 2, S'_{mp} = 0.7$		0.92/(1.82–2.78)
	Without notched band	1.13/(2.84–3.97)
		3.59/(0.41–4.00)

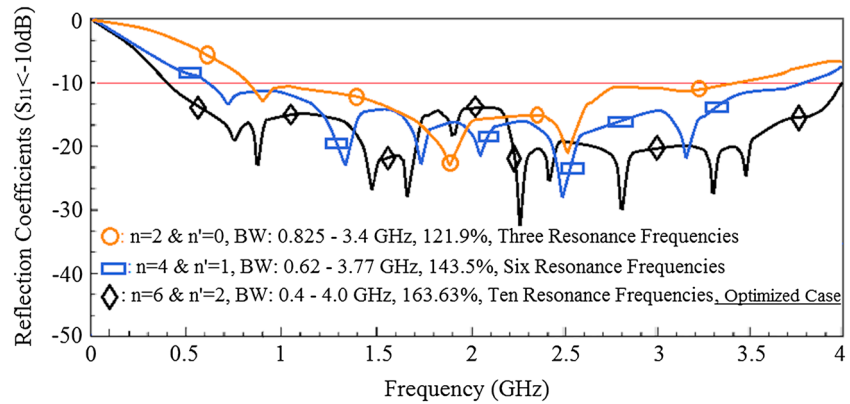
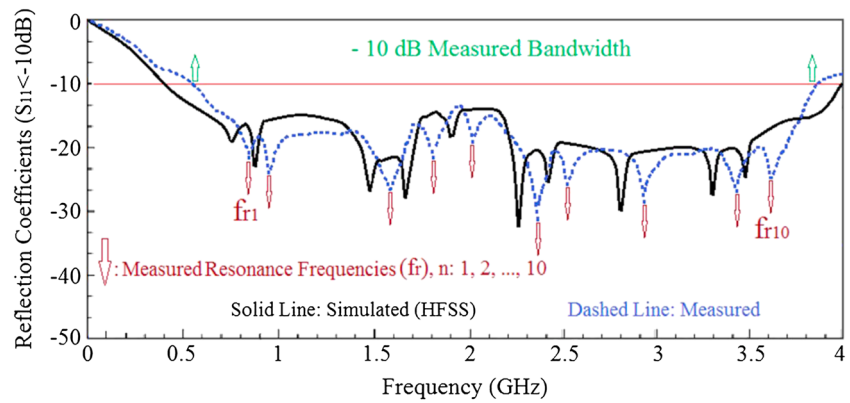
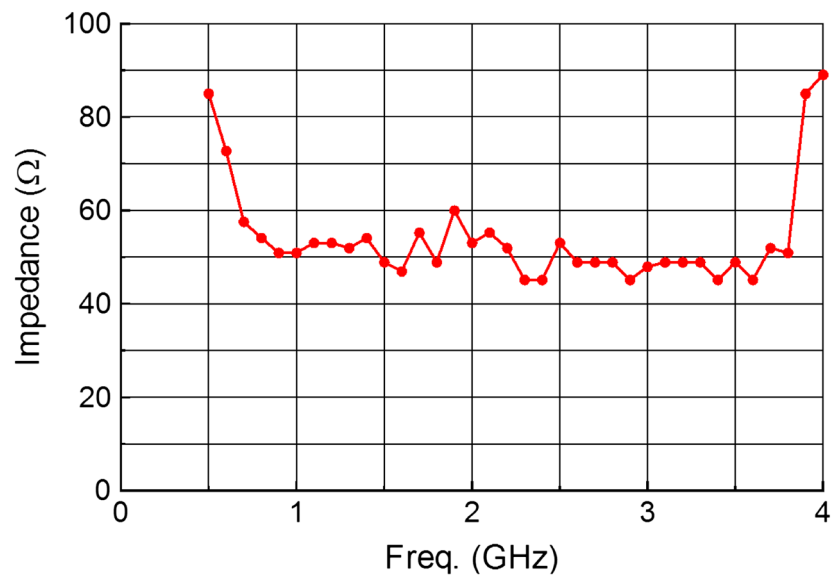


Figure 4. Reflection coefficient response of the proposed antenna as a function of number of meandered lines turns.



(a)



(b)

Figure 5. (a) Simulated and measured reflection coefficient response of the proposed meandered line antenna and (b) impedance match response of the antenna.

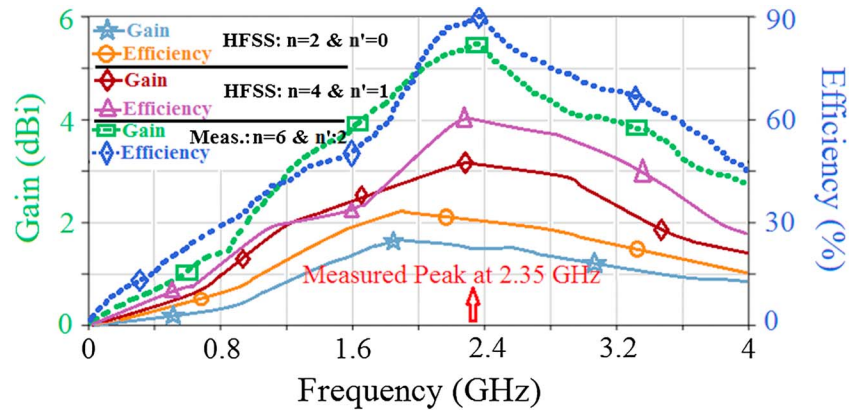


Figure 6. Gain and efficiency response of the proposed antenna as a function number of meandered lines turns.

The antenna resonates at 0.85, 0.95, 1.575, 1.8, 2.0, 2.35, 2.5, 2.9, 3.4, and 3.6 GHz. The antenna has a large impedance bandwidth (for $S_{11} < -10$ dB) spanning 550 MHz to 3.35 GHz, which corresponds to a fractional bandwidth of 150%. The impedance matching of the antenna, given in Figure 5b, shows the average impedance is 50.9Ω between 0.7 GHz to 3.8 GHz. These properties make it applicable for simultaneous use by numerous systems, such as JCDMA, Cellular, UHF RFID, GSM 900, GPS, KPCS, DCS, IMT-2000, WiMAX, lower band of WiFi, and Bluetooth bands.

The measured gain and radiation efficiency of meandered line antenna in Figure 6 shows it reaches a peak value of 5.5 dBi and 90.1%, respectively, at 2.35 GHz. Over its operational frequency from 550 MHz to 3.85 GHz the gain and efficiency remain better than 0.84 dBi and 21.1%. By increasing the number of turns in the meandered lines, the effective aperture of the antenna increases. As a consequence, the gain and efficiency performance improve significantly as shown in Figure 6. By using two turns in the meandered line with no interconnecting meandered line, maximum gain and efficiency were 1.65 dBi and 33%, respectively, at 1.9 GHz. Using four turns in the main meandered line and a single turn in the interconnecting line results in gain and efficiency of 3.15 dBi and 60%, respectively, at 2.3 GHz. The gain and efficiency have almost doubled. Using six turns in the main meandered line and two turns in the interconnecting line results in a maximum gain and radiation efficiency of 5.5 dBi and 90.1%, respectively, at 2.35 GHz. In this case the gain and efficiency have effectively tripled. The measured gains and efficiencies ranges are $0.84 \text{ dBi} \leq \text{Gain} \leq 5.5 \text{ dBi}$ and $21.1\% \leq \text{Efficiency} \leq 90.1\%$, respectively, over 550 MHz and 2.35 GHz. The gain and efficiency at various frequencies for $n = 6$ and $n' = 2$ is given in Table 3.

The current distribution over the antenna at various spot frequencies in its operational bandwidth is plotted in Figure 7. This reveals parts of the antenna that play a key role at the given frequency. Figure 8 shows the measured coradiation and cross-radiation patterns in E and H planes at various spot frequencies in the operational bandwidth of the antenna. It shows the antenna is omnidirectional in the E plane and essentially bidirectional in the H plane. The cross polarization is approximately -15 dB.

4. Conclusion

A compact planar antenna is proposed which is based on two pairs of meandered line loops that are interconnected to each other. The antenna's characteristics can be controlled by modifying the meandered line parameters. The measured results confirm the antenna covers a large bandwidth from 550 MHz to 3.85 GHz corresponding to a fractional bandwidth of 150%. It exhibits a peak gain and efficiency of 5.5 dBi and 90.1%, respectively, at 2.35 GHz and radiates omnidirectionally in the E plane. The proposed meandered antenna is easy to fabricate, and its low profile makes it suitable for wireless portables devices.

Table 3. Gain and Efficiency at Various Spot Frequencies

Frequency (GHz)	0.55	0.85	0.95	1.58	1.80	2.00	2.35	2.50	2.90	3.40	3.60	3.85
Gain (dBi)	0.84	1.50	1.85	3.75	4.25	4.95	5.50	5.05	4.23	3.85	3.25	2.93
Efficiency (%)	21.1	26.3	32.8	50.1	58.8	75.3	90.1	84.3	72.8	66.6	59.1	50.3

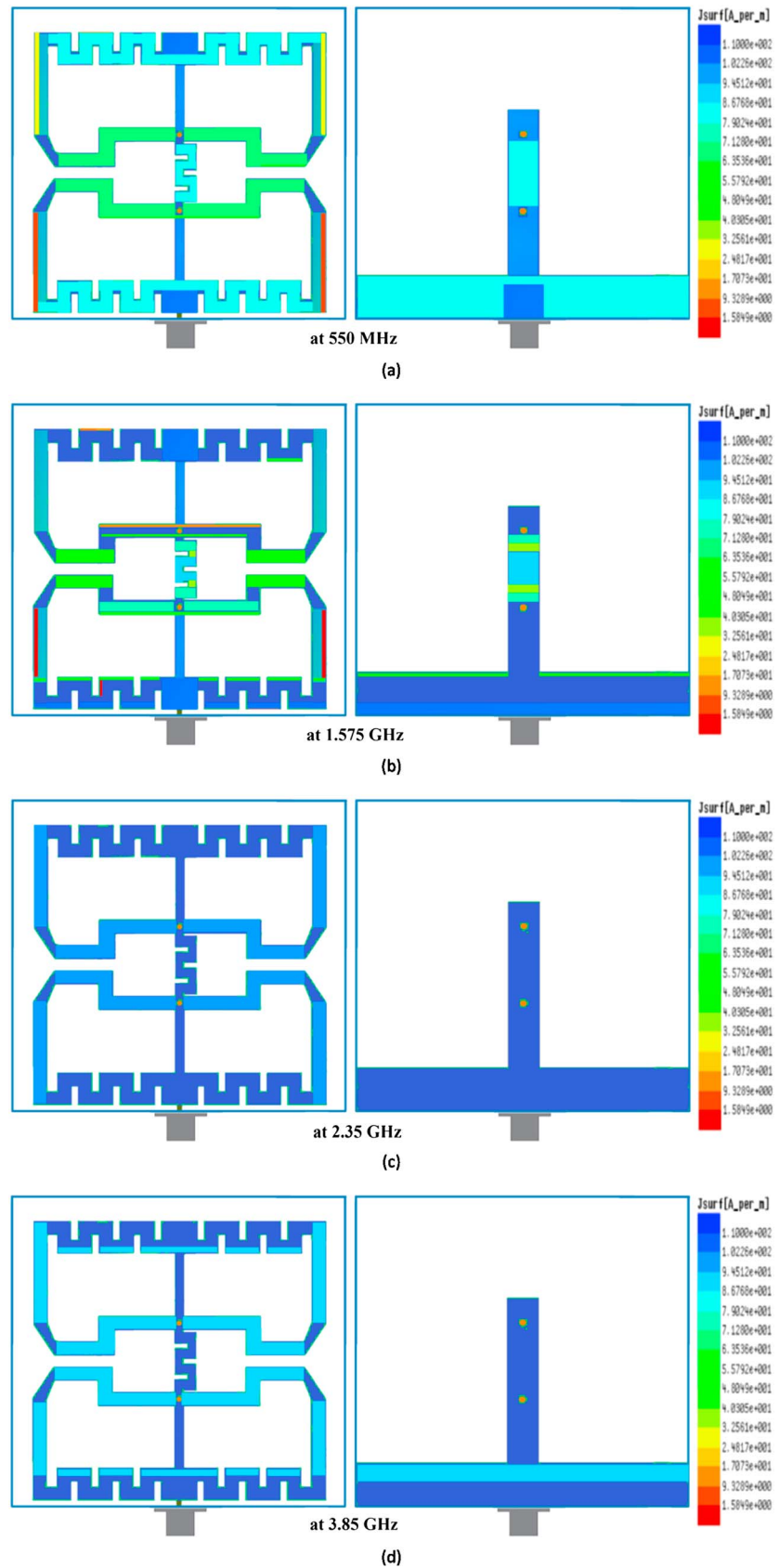


Figure 7. The current density distribution over the proposed antenna.

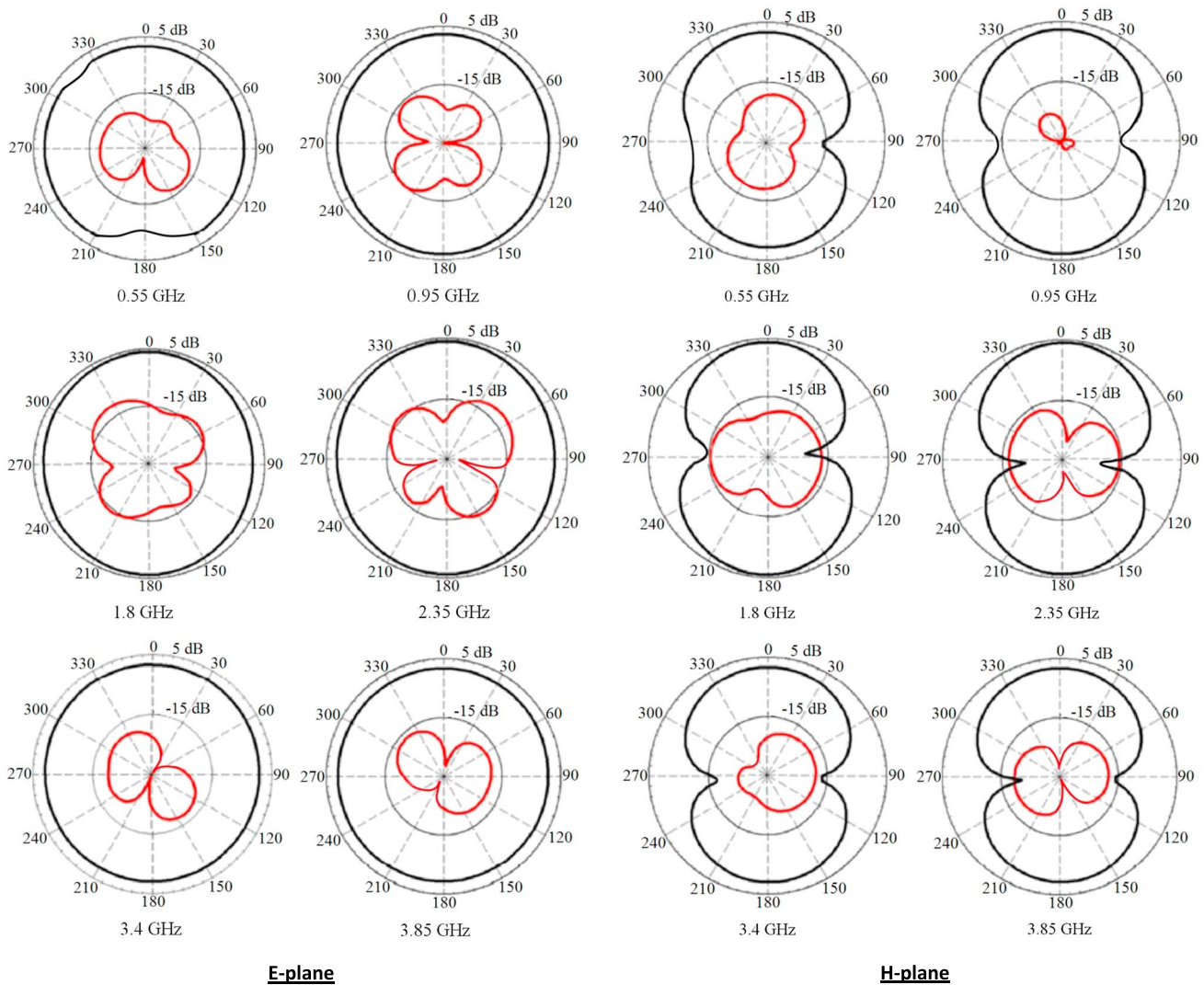


Figure 8. Measured coradiation (black line) and cross-radiation (red line) patterns in *E* and *H* planes of the proposed antenna at the various spot frequencies in the operational bandwidth of the antenna.

Acknowledgments

The data used are listed in the references, tables, and figures. For additional information, please contact Mohammad Naser-Moghadasi at mn.moghaddasi@srbiau.ac.ir.

References

Abutarboush, H. F., H. Nasif, R. Nilavalan, and S. W. Cheung (2012), Multiband and wideband monopole antenna for GSM900 and other wireless applications, *IEEE Antenn. Wireless Propagat. Lett.*, 11, 539–542.

Alibakhshi-Kenari, M., and M. Naser-Moghadasi (2015), Novel UWB miniaturized integrated antenna based on CRLH metamaterial transmission lines, *AEUE Int. J. Electron. Commun.*, 69(8), 1143–1149.

Alibakhshi-Kenari, M., M. Naser-Moghadasi, B. S. Virdee, A. Andújar, and J. Anguera (2015a), Compact antenna based on a composite right/left handed transmission line, *Microwave Optic. Technol. Lett.*, 57(8), 1785–1788.

Alibakhshi-Kenari, M., M. Naser-Moghadasi, and R. A. Sadeghzadah (2015b), Bandwidth and radiation specifications enhancement of monopole antennas loaded with split ring resonators, *IET Microwaves Antenn. Propagat.*, 9(14), 1487–1496.

Alibakhshi-Kenari, M., M. Naser-Moghadasi, and R. A. Sadeghzadeh (2015c), Composite right-left handed based-antenna with wide applications in very-high frequency–ultra-high frequency bands for radio transceivers, *IET Microw. Antenn. Propagat.*, 9(15), 1713–1726.

Alibakhshi-Kenari, M., M. Naser-Moghadasi, and R. A. Sadeghzadah (2015d), The resonating MTM based miniaturized antennas for wide-band RF-microwave systems, *Microwave Optic. Technol. Lett.*, 57(10), 2339–2344.

Alibakhshi-Kenari M., M. Naser-Moghadasi, R. A. Sadeghzadeh, B. S. Virdee, and E. Limiti (2016a), Bandwidth extension of planar antennas using embedded slits for reliable multiband RF communications, *AEU Int. J. Electron. Commun.*, 70(7), 910–919.

Alibakhshi-Kenari, M., M. Naser-Moghadasi, R. A. Sadeghzadeh, and B. S. Virdee (2016b), Metamaterial-based antennas for integration in UWB transceivers and portable microwave handsets, *Int. J. RF Microwave Comp. Aided Eng.*, 26(1), 88–96.

Alibakhshi-Kenari, M., M. Naser-Moghadasi, R. A. Sadeghzadeh, B. S. Virdee, and E. Limiti (2016c), New compact antenna based on simplified CRLH-TL for UWB wireless communication systems, *Int. J. RF Microwave Comput. Aided Eng.*, 26(3), 217–225.

Alibakhshi-Kenari, M., M. Naser-Moghadasi, R. A. Sadeghzadeh, B. S. Virdee, and E. Limiti (2016d), Dual-band RFID tag antenna based on the Hilbert-curve fractal for HF and UHF applications, *IET Circ. Device. Syst.*, 10(2), 140–146.

Alibakhshi-Kenari, M., A. Andújar, and J. Anguera (2016e), New compact printed leaky-wave antenna with beam steering, *Microwave Optic. Technol. Lett.*, 58(1), 215–217.

- Alibakhshi-Kenari, M., M. Naser-Moghadasi, R. A. Sadeghzadeh, and B. S. Virdee (2016f), Hexa-band planar antenna with asymmetric fork-shaped radiators for multiband and broadband communication applications, *IET Microwaves Antenn. Propagat.*, 10(5), 471–478.
- Balanis, C. A. (1997), *Antenna Theory: Analysis and Design*, 2nd ed., John Wiley, New York.
- Chien, H. Y., C. Y. D. Sim, and C. H. Lee (2013), Dual-band meander monopole antenna for WLAN operation in laptop computer, *IEEE Antenn. Wireless Propagat. Lett.*, 12, 694–697.
- Du, Z., Z. Wu, M. Wang, J. Rao, and P. Luo (2015), Compact quasi-Yagi antenna for handheld UHF RFID reader, *ACES J.*, 30(8), 860–865.
- Lee, J.-N., J.-D. Park, K.-C. Lee, and J.-K. Park (2014), Design of a meander dipole antenna with dielectric loading for a sensor node of a wireless sensor network, *Microw. Optic. Technol. Lett.*, 56(7), 1526–1531.
- Li, Y., W. Li, and R. Mittra (2013), A compact ACS-fed dual-band meandered monopole antenna for WLAN and WiMAX applications, *Microw. Optic. Technol. Lett.*, 55(10), 2370–2373.
- Ojaroudi, N., M. Ojaroudi, and K. Halili (2012), Design of triple band monopole antenna with meander line structure for MIMO application, *Microw. Optic. Technol. Lett.*, 54(9), 2168–2172.
- Pandeeswari, R., and S. Raghavan (2015), Meandered CPW-fed hexagonal split-ring resonator monopole antenna for 5.8 GHz RF-ID applications, *Microw. Optic. Technol. Lett.*, 57(3), 681–684.
- Sharma D., and M. S. Hashmi (2014), A novel design of tri-band patch antenna for GSM/WiFi/WiMAX applications, IEEE MTT-S International Microwave and RF Conference (IMaRC), Bangalore, India, pp. 156–158, Dec. 2014.